CELL CYCLE
2023, VOL. 22, NO. 17, 1865–1883
https://doi.org/10.1080/15384101.2023.2244778

Taylor & Francis
Taylor & Francis Group

RESEARCH PAPER

SNTB1 regulates colorectal cancer cell proliferation and metastasis through YAP1 and the WNT/β-catenin pathway

Hao Zhang[a*], Zheng Li[a*], Juan Jiang[b], Yang Lei[a], Jingmao Xie[a], Yihui Liu[a], and Bo Yi[a]

[a]Department of Gastrointestinal Surgery, the Third Xiangya Hospital, Central South University, Changsha, China; [b]Department of Nephrology, the Third Xiangya Hospital, Central South University, Changsha, China

ABSTRACT

Colorectal cancer is a common type of digestive tract cancer with a significant morbidity and death rate across the world, partially attributing to the metastasis-associated problems. In this study, integrative bioinformatics analyses were performed to identify genes that might contribute to colorectal cancer metastasis, and 293 genes were dramatically increased and 369 genes were decreased within colon cancer samples. Among up-regulated genes, top five genes correlated with colorectal cancer patient's prognosis were verified for expression in clinical samples and syntrophin beta 1 (SNTB1) was the most up-regulated. *In vitro*, SNTB1 knockdown suppresses the malignant behaviors of colorectal cancer cells, including cell viability, colony formation capacity, as well as the abilities to migrate and invade. Furthermore, SNTB1 knockdown decreased the levels of Wnt1, C-Jun, C-Myc, TCF7, and cyclin D1, and inhibited EMT in both cell lines. *In vivo*, SNTB1 knockdown inhibited tumor growth and metastasis in nude mice models. SNTB1 positively regulated Yes1 associated transcriptional regulator (YAP1) expression; YAP1 partially reversed the effects of SNTB1 on colorectal cancer cell phenotypes and the Wnt/β-catenin/MYC signaling. In conclusion, SNTB1 knockdown inhibits colorectal cancer cell aggressiveness *in vitro* and tumor growth and metastasis *in vivo* through the Wnt/β-catenin/MYC signaling; YAP1 might mediate SNTB1 functions on colorectal cancer.

ARTICLE HISTORY
Received 2 April 2023
Revised 30 May 2023
Accepted 15 June 2023

KEYWORDS
Colorectal cancer; metastasis; SNTB1; YAP1; the Wnt/β-catenin/MYC signaling

Introduction

Colorectal cancer is a common type of digestive tract cancer with a significant morbidity and death rate across the world [1]. Metastasis has a significant impact on the survival rate of patients, and metastasis-associated problems constitute the leading cause of cancer mortality [2]. About 15–25% of colorectal cancer patients develop hepatic metastases, resulting in a worse prognosis [3]. Metastasis is a complex process that involves the spread of a tumor or cancer to distant parts of the body from its original site through the blood or lymph system.

Numerous researchers have found the essential role of epithelial–mesenchymal transition (EMT) within the invasion and metastasis of colorectal cancer [4,5]. During EMT, epithelial tumor cells undergo unique morphological and phenotypic alterations, such as loss of tight junctions, cell polarity, and cytoskeletal rearrangement, resulting in cells with more invasive capabilities and morphologies [6,7]. Key proteins that regulate EMT include E-cadherin, N-cadherin, vimentin, and tight junction protein 1 (ZO-1) [8]. Furthermore, zinc finger E-box-binding homeobox 1 (ZEB1) and SMAD family member 3 (SMAD3) may function as transcription factors in the regulation of EMT [9]. Potential ways to controlling CRC metastases include strategies for precisely controlling the EMT process.

Signaling pathways, including nuclear factor-kappa B (NF-κB) pathway [10], transforming growth factor β (TGF-β) pathway [11], Notch pathway [12], and Wnt/β-catenin pathway [13] are known to be implicated in the acceleration of EMT and tumor metastasis. Being constitutively activated during cancer progression, the canonical Wnt/β-catenin pathway has become one of the most prominent molecular therapeutic targets for colon cancer [14] because of its critical role in

CONTACT Bo Yi xy3yygs3@163.com Department of Gastrointestinal Surgery, the Third Xiangya Hospital, Central South University, No. 138 Tongzipo Road, Yuelu District, Changsha City, Hunan Province, China
*The author contribute equally to this study.
Supplemental data for this article can be accessed online at https://doi.org/10.1080/15384101.2023.2244778

accelerating EMT and facilitating metastatic features of colon cancer [15]. Following the Wnt signaling activation, β-catenin translocates into and accumulates in the nucleus [16], where β-catenin binds to T cell factor (TCF), subsequently trans-activating target genes through TCF-binding elements (TBEs) [17,18]. Importantly, β-catenin accumulation in the nucleus is observed in up to 80% of colon cancer patients [15,19]. As a result, future research into new regulators of Wnt/β-catenin pathway and underlying processes may aid in the development of antimetastatic treatments for colon cancer.

In this study, integrative bioinformatics analyses were performed to identify differentially expressed genes that represent risk factors for colorectal cancer and SNTB1 was chosen. The *in vitro* effects of SNTB1 upon the malignant behaviors of cancer cells and *in vivo* effects of SNTB1 upon tumor growth and metastasis in nude mice models were investigated. Furthermore, the effects of SNTB1 on the Wnt/β-catenin/MYC signaling and EMT markers were evaluated. Regarding downstream molecular mechanism, SNTB1 knockdown was achieved in colorectal cancer HCT116 cells, RNA sequencing was performed identifying correlated genes that might mediate SNTB1 functions on colorectal cancer phenotypes, and YAP1 was selected. SNTB1 regulation of YAP1 and the dynamic effects of SNTB1 and YAP1 on colorectal cancer cells, the Wnt/β-catenin/MYC signaling, and EMT markers were investigated. Collectively, this study aims to provide a solid experimental basis for identifying novel therapeutic targets for metastatic colorectal cancer.

Materials and methods

Clinical sample collection

Ten pairs of colorectal cancer and matched adjacent non-cancerous tissue specimens were obtained from colorectal cancer patients undergoing resection. After staining with hematoxylin and eosin (H&E) for histopathological features, all specimens were kept at −80°C until further use. Informed consent form was signed by each patient involved. The whole sample collection was conducted under the approval of the Third Xiangya Hospital of Central South University.

Hematoxylin and eosin (H&E) staining

Tissues were preserved in 4% paraformaldehyde (PFA) overnight before being processed and embedded in paraffin. Sections (5-μm in sickness) were cut and stained as directed by the manufacturer's protocols. A microscope (Olympus, Tokyo, Japan) was applied to photograph the stained slices.

Immunohistochemical staining (IHC)

After deparaffinization in xylene, tissue slices were rehydrated in a graduated ethanol series. Slices were immersed for 30 min in 0.3% H_2O_2 in peroxidase–methanol solution to inactivate endogenous peroxidase activity. Slices for antigen retrieval were immersed in sodium citrate buffer, and heated in a microwave for 15 min at 100°C. Tissue slices were hybridized overnight at 4°C with anti-SNTB1 (AB242046, Abcam, Cambridge, MA, USA), and an UltraVision Quanto Detection System HRP DAB Kit (Thermo Scientific, Shanghai, China) was utilized to perform further steps per the manufacturer's instructions. After hematoxylin counterstaining, a microscope (Olympus, Tokyo, Japan) was employed to photograph the slices. Expression densities of the SNTB1 protein were measured by ImageJ software.

Cell lineages and cell culture

The normal colon epithelial cell line NCM460 (M-C1287, CellBank. Australia) were cultured in RPMI-1640 medium (30–2001, ATCC) containing with 10% FBS (Gibco). A colon cancer cell line SW480 (CCL-228, ATCC) cultivated in Leibovitz's L-15 Medium (30–2008, ATCC) containing 10% FBS (Gibco). A colon cancer cell line HCT 116 (CCL-247, ATCC) cultivated in McCoy's 5A Medium (30–2007, ATCC) containing with 10% FBS (Gibco). A colon cancer cell line HCT8(CCL-244, ATCC) cultivated in RPMI-1640 medium (30–2001, ATCC) containing with 10% FBS (Gibco). A colon cancer cell line LoVo (ATCC, CCL-229) cultivated in F-12K Medium (ATCC, 30–2004) containing with 10% FBS (Gibco). A colon cancer cell line DLD-1 (ATCC, CCL-221) cultivated in RPMI-1640 medium (30–2001,

ATCC) containing with 10% FBS (Gibco). All cell types were cultivated at 37°C in a humidified atmosphere containing 5% CO_2.

Cell transduction

Short hairpin RNA targeting SNTB1 (sh-SNTB1#1/2; GenePharma, Shanghai, China) was transfected to achieve SNTB1 knockdown in target cells. Plasmid overexpressing YAP1 (YAP1; GenePharma) was transfected to achieve YAP1 overexpression in target cells. Cells were transfected using Lipofectamine 3000 reagent (Invitrogen, Carlsbad, CA, USA). The transfection media was discarded 6 h following transfection. Forty-eight hours later, cells were harvested for further investigation. The primers for vector construction are listed in **Table S1**.

CCK-8 detecting cell viability

For cell viability determination, 3000 viable cells per well were seeded onto 96-well plates for 48, 72 h, then, 10 µl Cell Counting Kit solution (Beyotime, China) was supplemented, followed by the incubation of the 96-well plates at 37°C for 4 h. The OD value at 490 nm was measured by a microplate reader.

Plate clone formation assay

Target cells were cultured in a six-well plate (6×10 [2] cells/well) for 14 days. The cultured media was refreshed every 4 days. After that, cells were fixed in 4% formaldehyde and stained with crystal violet. Cell clones were counted and examined.

Wound healing assay for cell migration

Cells were cultured in a six-well plate until 70% confluency was reached. The media in each well was refreshed 4 h following transduction. After 24 h, a scratch was made vertically at the center of the well using a pipette tip. Wound regions were photographed at 0 h, and the medium was replaced on a regular basis for up to 48 h, when the wound regions were photographed again. Wound regions were measured and compared using the Image J software.

Transwell assay for cell invasion and migration

Transwell was used to examine cancer cell invasion (pre-coated with Matrigel) and migration (non-coated with Matrigel). Matrigel (1:8 diluent of 50 mg/L) was coated on the upper surface of the bottom membrane of the Transwell chamber and dried at 4°C for the invasion assay, and Transwell chamber without pre-coated Matrigel was used for the migration assay. Cell suspension (200 µL) was obtained and placed into the Transwell chamber (1×10 [5] cells in each chamber) and cultivated for 24 h. Invaded or migrated cells on the lower surface of the bottom chambers were fixed and observed under an inverse microscope.

Immunofluorescence (IF) staining

Primary antibodies against E-Cadherin (ab231303, Abcam), Vimentin (ab20346, Abcam) and FITC-labeled goat anti-mouse or rabbit IgG as the secondary antibody were used in IF staining for detecting the levels of E-cadherin and Vimentin. Briefly, transfected cells were seeded on coverslips for 24 h. Then, wash the cells with PBS, fix them in 4% paraformaldehyde, permeabilize the cells in 0.1% TritonX-100, and block in PBS buffer containing 5% bovine serum albumin for 30 min at room temperature. The cell coverslips were further incubated with primary antibody (1:200, 4°C overnight) and FITC-labeled secondary antibody (1:400, room temperature for 2 h). Finally, the fluorescent signals were observed by fluorescence microscope (Olympus).

Elisa

According to manufacturer instructions, corresponding ELISA kits (all purchased from RUIXIN Biotech, Quanzhou, China) were employed to examine CXCL9, CXCL10, and CXCR3 levels in the sh-NC or sh-SNTB1#1/2 transfected HCT116 and SW480 cells.

Immunoblotting

RIPA was used to lyse the cells, and total protein was collected. After electrophoresis with 10% SDS-PAGE, the separated proteins (50 μg) from the gel were transferred onto PVDF membranes, and 5% skim milk in TBST was used to block protein samples for 1 h at ambient temperature. After that, the membranes were treated with primary antibodies against SNTB1 (AB242046, Abcam), Wnt1 (ab15251, Abcam), C-jun (ab40766, Abcam), C-myc (10828–1-AP, Proteintech), TCF7 (CSB-PA004247, CSUBIO, China), Cyclin D1 (ab16663, Abcam), E-Cadherin (ab231303, Abcam), N-Cadherin (ab76011, Abcam), Vimentin (ab20346, Abcam), Snail (CSB-PA004123, CSUBIO), Slug (ab27568, Abcam), MMP9 (ab283575, Abcam) and GAPDH (ab8245, Abcam) and cultured at 4°C overnight, followed by treatment with the secondary antibody for 1 h at room temperature. An enhanced chemiluminescence reagent (Beyotime) was employed to visualize the blot bands. The gray density was analyzed by ImageJ software (NIH, USA).

qRT-PCR

Following the manufacturer's directions, the TRIzol Reagent (Invitrogen, Waltham, MA, USA) was employed to extract total RNA from target tissues and cells. mRNA levels were measured using PrimeScript RT reagent Kit with gDNA Eraser and TB Green Premix Ex Taq II (Takara, Dalian, China). GAPDH was used to standardize all of the data. The relative expression of mRNAs was calculated using the $2^{-\Delta\Delta Ct}$ method. The primers for qRT-PCR assay were listed in **Table S1**.

Experimental animals

Five-week-old male BALB/c nude mice were procured from SLAC laboratory animal company (Changsha). Mice were kept in specific-pathogen-free conditions and permitted ad libitum access to drinking water and food according to the Animal Care Committee of the Third Xiangya Hospital of Central South University.

Subcutaneous xenotransplanted tumor model in nude mice

Stably transfected HCT-116 cells (infected with Lv-sh-SNTB1#1/2) were injected into the mice's flank ($n = 6$). The sizes of the xenografts were gauged on a weekly basis (calculated volume = shortest diameter2 *longest diameter/2). At day 25, the subcutaneous tumors were collected and measured and weighed. Following that, tumor tissues were paraffin-embedded for H&E staining, IHC staining, and Immunoblotting.

In vivo metastasis assay

The nude mice were tail-vein injected with the specified number of stably transfected HCT-116 cells (transfected with Lv-sh-SNTB1#1/2; 3×10^6/0.2 ml PBS). After 25 days, all mice were sacrificed under anesthesia, and their lungs were surgically dissected and collected. The lung tissues were paraffin-embedded for H&E staining, IHC staining, Immunoblotting, and statistical analysis of tumor nodule number.

RNA sequencing

HCT116 cells were infected with sh-NC lentivirus or sh-SNTB1#1 lentivirus for 48 h and collected for RNA sequencing. Briefly, the total RNA was isolated by Trizol (Invitrogen). The RNA concentration and quality were determined by a Nano Drop and Agilent 2100 Bioanalyzer (Thermo Fisher, USA). The mRNA library construction was performed on BGIseq500 platform according to previous description [20]. The sequencing data was filtered with SOAPnuke (v1.5.2) [21] then clean reads were obtained and stored in FASTQ format. The clean reads were mapped to the reference genome using HISAT2 (v2.0.4) [22]. Bowtie2 (v2.2.5) [23] was applied to align the clean reads to the reference coding gene set, then expression level of gene was calculated by RSEM (v1.2.12) [24]. The heatmap was drawn by R language clusterprofiler package [25] according to the gene expression in different samples. The differernt expression genes were analyzed using the DESeq2(v1.4.5) [26] with log2fc > 0.4 or <-0.4 and Q value ≤ 0.05. To take insight to the change of phenotype, GO

(http://www.geneontology.org/) and KEGG (https://www.kegg.jp/) enrichment analysis of annotated different expressed gene was performed by Phyper (https://en.wikipedia.org/wiki/Hypergeometric_distribution) based on Hypergeometric test. The significant levels of terms and pathways were corrected by Q value with a rigorous threshold (Q value ≤ 0.05) by Bonferroni [27].

Statistical analysis

The animal experiments were implemented six independent times at lowest. The cell experiments were implemented for three independent times at lowest. The statistical tool SPSS version 21.0 (SPSS Inc., New York, NY, USA) was used for all statistical analyses. To compare differences between groups, the two-tailed paired Student's *t*-test was utilized. Survival curves were plotted using the Kaplan–Meier approach, and survival curves were compared using the log-rank test. Survival data were analyzed using univariate and multivariate Cox regression models. A P-value of 0.05 or less was judged statistically significant.

Results

Bioinformatics analyses screening for key differentially expressed genes (DEGs) in colorectal cancer

For identifying DEGs between colorectal cancer and non-cancerous normal samples, four datasets were downloaded and analyzed. GSE39582 contains expression profiles of 566 colon cancer cases and 19 normal intestinal mucosa samples; 22189 genes were detected and 2034 differential genes were obtained, with 1082 genes decreased (log2FC < −1, $P < 0.05$) and 952 were increased (log2FC > 1, $P < 0.05$) in tumor tissues. GSE8671 contains expression profiles of 32 colorectal adenomas and normal mucosal samples; 22189 genes were detected and 2388 differential genes were obtained, with 1410 genes decreased (log2FC < −1, $P < 0.05$) and 978 genes increased in tumor tissue (log2FC > 1, $P < 0.05$). GSE44076 contains paired tumor samples and normal adjacent mucosa from a cohort of 98 patients and 50 healthy colon mucosae; 20034 genes were detected and 2354 differential genes were obtained, with 1250 genes decreased (log2FC < −1, $P < 0.05$) and 1104 genes increased in tumor tissues (log2FC > 1, $P < 0.05$). GSE9348 contains 70 samples from patients with early colorectal cancer and 12 normal mucosal samples from healthy controls; 22189 genes were detected and 3540 differential genes were obtained, with 1751 down-regulated (log2FC < −1, $P < 0.05$) and 1789 up-regulated in tumor tissues (log2FC > 1, $P < 0.05$) (Figure 1a-b). Overlapped increased/decreased genes in colorectal cancer according to the four datasets were shown; 293 genes were dramatically increased and 369 genes were decreased within cancer samples according to all four sets of datasets (Figure 1c-d).

Moreover, as for correlated signaling pathways and functions of these DEGs, KEGG signaling enrichment annotation and PPI analysis were performed. Up-regulated genes were enriched in common tumor proliferation and apoptosis-related pathways, microRNAs in cancer, cell cycle, TP53 signaling pathway, and Interleukin 17 (IL-17) family-mediated signaling pathways (Figure 2a-b). IL-17 is a pleiotropic pro-inflammatory cytokine that promotes cancer-induced inflammation and allows cancer cells to undergo immunosurveillance escape [28]. Downregulated genes were enriched in metabolic pathways such as nitrogen metabolism, steroid hormone biosynthesis, retinol metabolism, mineral absorption, bile secretion, and pancreatic secretion (Figure 2c-d), indicating the loss of colon functions during colorectal cancer.

SNTB1 is up-regulated in colorectal cancer and correlated with worse prognosis in patients

For identifying risk factors for colorectal cancer, the Cox univariate regression analysis was performed on 369 down-regulated genes and 293 up-regulated genes with the Survival and SurvMiner packages in the R language. Fig.3a shows that 31 up-regulated genes were linked to colorectal cancer patients' overall survival, representing risk factors (Hazard Ratio > 1, $P < 0.05$). For narrowing the range of risk factors, the expression levels of the top five risk factors (FKBP10, SFTA2,

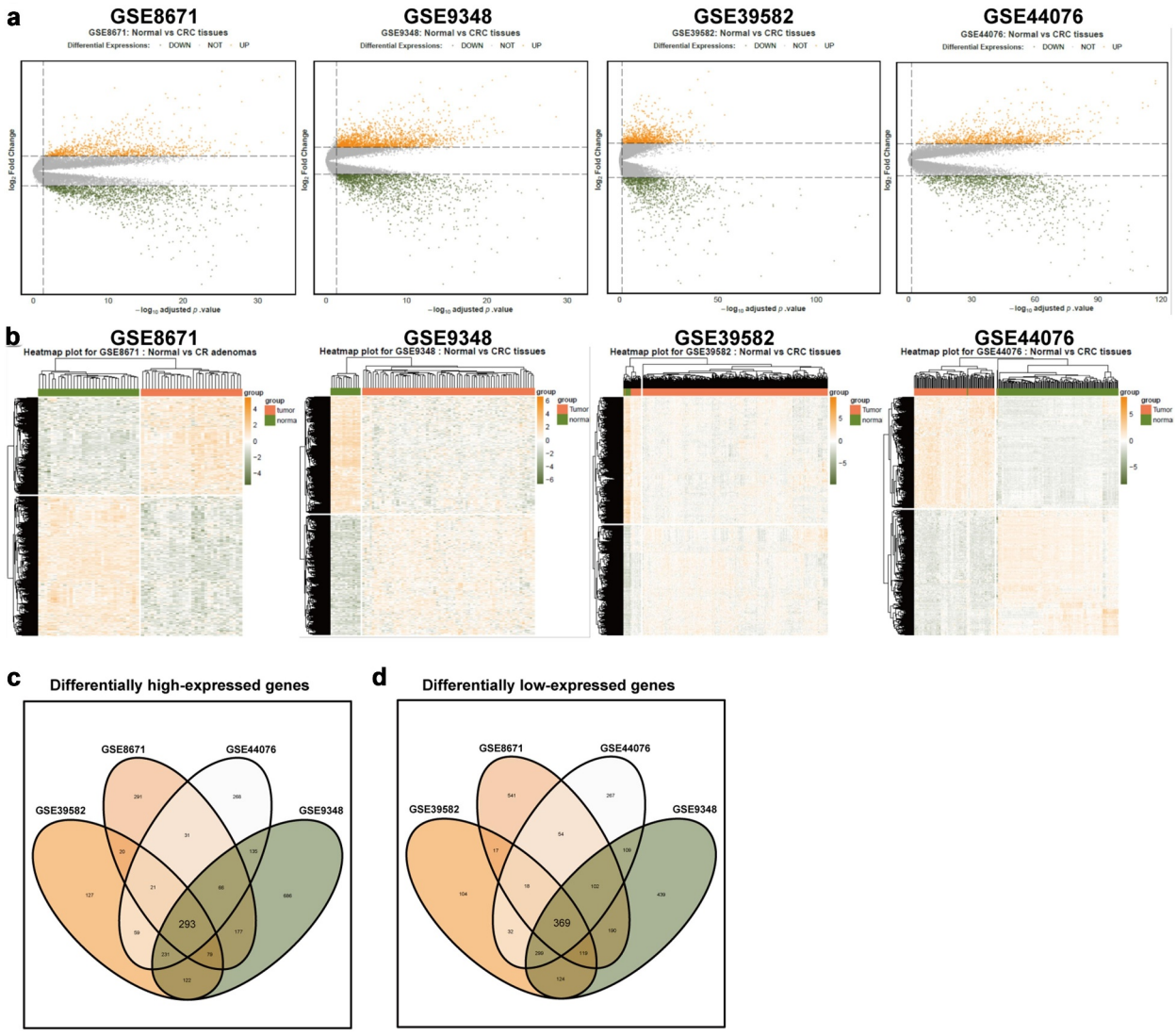

Figure 1. Bioinformatics analyses screening for key differentially expressed genes (DEGs) in colorectal cancer (a) Volcano plots showing differentially expressed genes between colorectal cancer and non-cancerous control samples according to GSE8671, GSE9348, GSE39582, and GSE44076. (b) Hierarchical clustering heatmap showing differentially expressed genes between colorectal cancer and non-cancerous control samples according to GSE8671, GSE9348, GSE39582, and GSE44076. (c-d) Overlapped up-regulated/down-regulated genes in colorectal cancer according to the four datasets.

TIMP1, STC1, and SNTB1) were examined in 10 pairs of colorectal cancer and matched adjacent non-cancerous samples; Figure 3b shows that FKBP10, TIMP1, STC1, and SNTB1 were remarkably increased in tumors, SNTB1 dramatically up-regulated. According to TCGA-COADREAD, GSE24514, GSE39582, GSE44076, GSE8671, and GSE9348, the expression level of SNTB1 showed to be markedly increased within tumors than control samples (Figure 3c-d). According to TCGA-COADREAD, SNTB1 expression was higher in tumor samples in advanced N/M/T stages and pathological stages (Figure 3e-h). Therefore, SNTB1 was chosen for following experimental analyses. Clinical colorectal cancer and matched adjacent para-cancerous tissues were collected and verified for the histopathological features using H&E staining (Figure 3i). SNTB1 levels were significantly elevated in collected clinical colorectal cancer samples compared with the non-cancerous samples, as revealed by IHC staining (Figure 3i). As further evidence, qRT-PCR and Immunoblotting were employed to examine SNTB1 mRNA and protein expression within collected clinical samples, respectively; Figure 3j-k shows that SNTB1

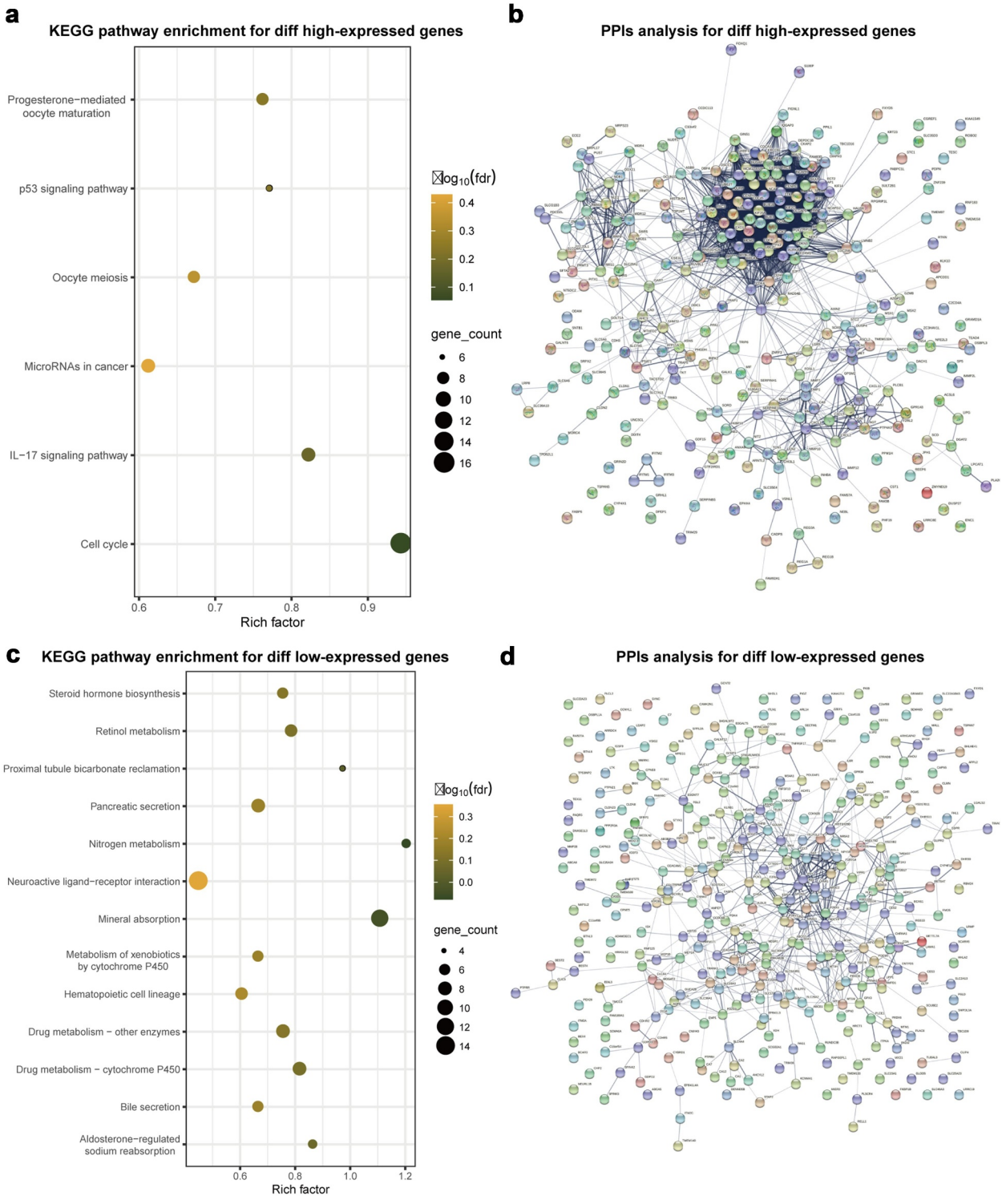

Figure 2. Kyoto Encyclopedia of Genes and Genomes (KEGG) and Protein–Protein Interaction (PPI) analyses (a-b) Up-regulated genes were applied for KEGG signaling enrichment annotation and PPI analysis. (c-d) Down-regulated genes were applied for KEGG signaling enrichment annotation and PPI analysis.

mRNA and protein expression were remarkably up-regulated within cancer samples than normal samples. TCGA-COADREAD cases were allocated into high-/low-SNTB1 expression groups taking the median value as the cutoff and examined for the relationship between SNTB1 level and the overall survival in patients using Cox univariate regression analysis. Figure 3l shows

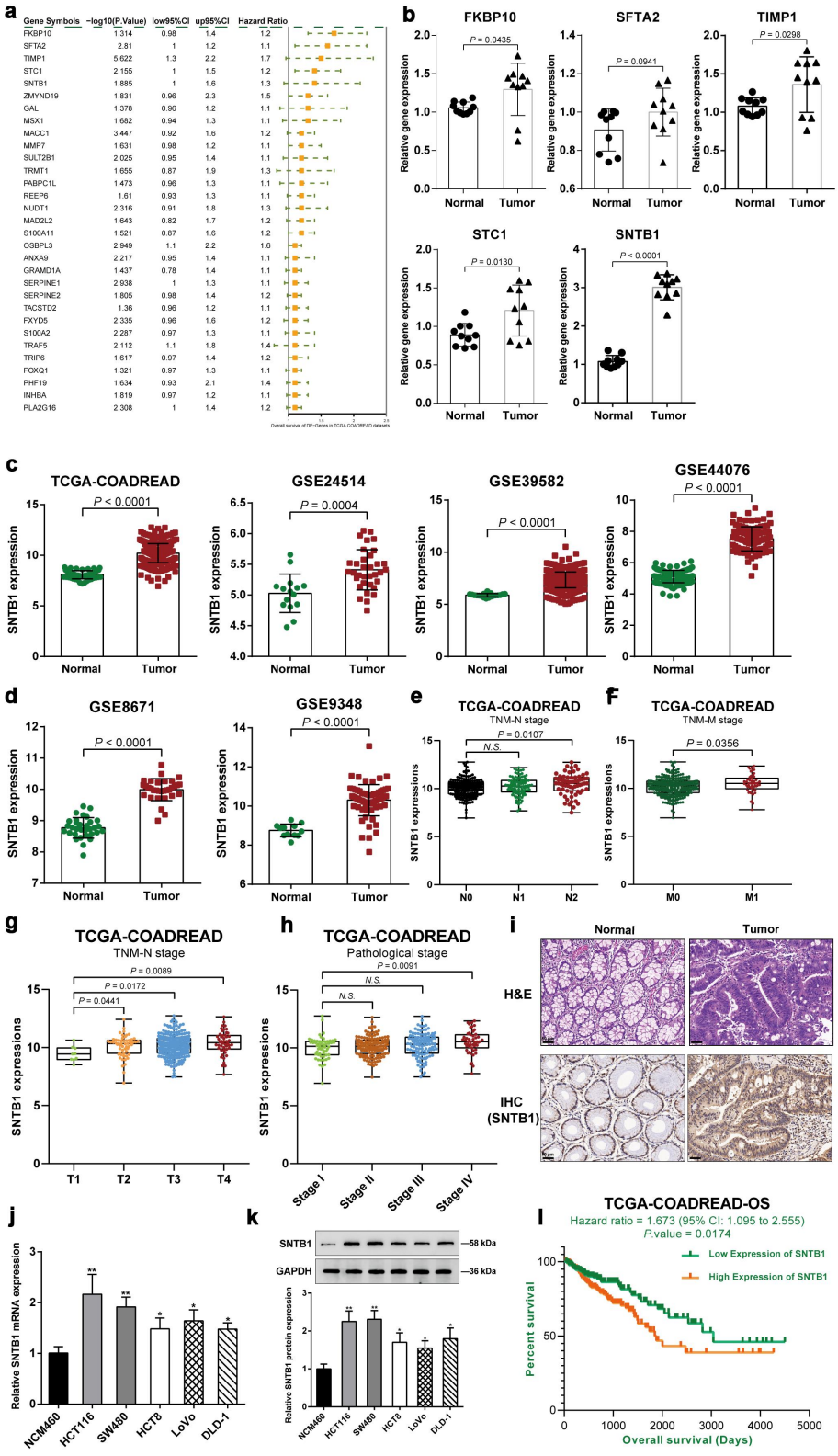

Figure 3. SNTB1 is up-regulated in colorectal cancer and correlated with worse prognosis in patients (a) Cox univariate regression analysis was performed on 369 down-regulated genes and 293 up-regulated genes using the Survival and SurvMiner packages in the R language. (b) Ten pairs of colorectal cancer and matched adjacent non-cancerous samples were collected and examined for the expression of the top five risk factors using Qrt-PCR. (c-d) SNTB1 expression in cancer and non-cancerous samples according to TCGA-COADREAD, GSE24514, GSE39582, GSE44076, GSE8671, and GSE9348. (e-h) SNTB1 expression in cancer samples of different N/M/T stages and pathological stages according to TCGA-COADREAD. (i) the histopathological characteristics and SNTB1 levels in collected clinical samples were evaluated using H&E and IHC staining, respectively. (j-k) the mRNA expression and protein levels of

that higher SNTB1 expression was associated with colorectal cancer patients' poorer overall survival. Therefore, SNTB1 might serve as an oncogenic factor in colorectal cancer.

Effects of SNTB1 knockdown on colorectal cancer cell phenotypes

For investigating the specific effects of SNTB1 upon colorectal cancer cells, sh-SNTB1#1/2 was transfected to achieve SNTB1 knockdown in target cells, as confirmed by qRT-PCR (Figure 4a). Subsequently, HCT116 and SW480 cells were transduced with sh-SNTB1#1/2 and examined for cell phenotypes. As speculated, SNTB1 knockdown by sh-SNTB1#1/2 significantly inhibited colorectal cancer cell viability (Figure 4b), colony formation (Figure 4c), cell migration (Figure 4d-e), and cell invasion (Figure 4f). Therefore, SNTB1 knockdown suppresses the malignant behaviors of colorectal cancer cells.

SNTB1 modulates the Wnt/β-catenin/MYC signaling and EMT

For identifying signaling pathways and factors involved in SNTB1 functions on colorectal cancer cells, SNTB1 co-expressed genes were analyzed based on 20,530 genes in the TCGA-COADREAD expression matrix containing 434 samples was analyzed using the R language PSYCH package and Pearson's correlation analysis. Fig 5a shows that SNTB1 co-expressed genes were negatively enriched in inflammatory response and immune regulation (interferon-α/γ, IFN-α/γ response) ($P < 0.05$), positively enriched in the Wnt/β-catenin pathway and Hedgehog pathway related to proliferation, and negatively enriched in apoptosis-associated process. Figure 5b shows that cell proliferation and migration-correlated Wnt/β-catenin signaling, MYC_Targets_V1 pathway, and MYC_Targets_V2 pathway were significantly up-regulated, whereas the apoptosis pathway was significantly down-regulated.

Therefore, HCT116 and SW480 cells were transduced with sh-SNTB1#1/2 and examined for the alterations in the Wnt/β-catenin/MYC signaling and migration-associated EMT. As for the Wnt/β-catenin/MYC signaling, SNTB1 knockdown by sh-SNTB1#1/2 significantly decreased the levels of Wnt1, C-Jun, C-Myc, TCF7, and cyclin D1 in both cell lines (Figure 5c). As for EMT markers, SNTB1 knockdown by sh-SNTB1#1/2 significantly up-regulated E-cadherin but down-regulated N-cadherin, Vimentin, Snail, Slug, and MMP-9 (Figure 5d-f). In summary, SNTB1 inhibits the Wnt/β-catenin/MYC pathway and EMT in colorectal cancer cells.

In vivo effects of SNTB1 on tumor growth and metastasis in mice models

After confirming the *in vitro* effects of SNTB1, we established subcutaneous xenotransplanted tumor model and metastatic tumor model in nude mice and investigated the *in vivo* effects of SNTB1. HCT116 cells transduced with Lv-sh-NC or Lv-sh-SNTB1#1/2, and the transfection efficiency was measured using qRT-PCR (Figure 6a). Then, the transfected HCT116 cells were injected into the flank of the mice. Figure 6b-c shows that SNTB1 knockdown dramatically reduced tumor volume and weight, and the appearance of the tumors is shown in Figure 6d. H&E staining was performed to further confirm the histopathological features (Figure 6e). Furthermore, IHC staining shows that the levels of SNTB1 and Ki67 were significantly decreased in tumor tissue samples (Figure 6e). Regarding the Wnt/β-catenin/MYC signaling, SNTB1 knockdown significantly decreased Wnt1, C-Jun, C-Myc, TCF7, and cyclin D1 protein contents in tumor tissue samples (Figure 6f). These data indicate that SNTB1 knockdown inhibits tumor growth in subcutaneous xenotransplanted tumor models.

Metastatic tumor model was established by tail vein injection of HCT116 cells transduced

SNTB1 in collected clinical samples were examined using Qrt-PCR and Immunoblotting, respectively. (l) Cox univariate regression analysis was performed on TCGA-COADREAD cases identifying the correlation between SNTB1 expression and the overall survival in patients.

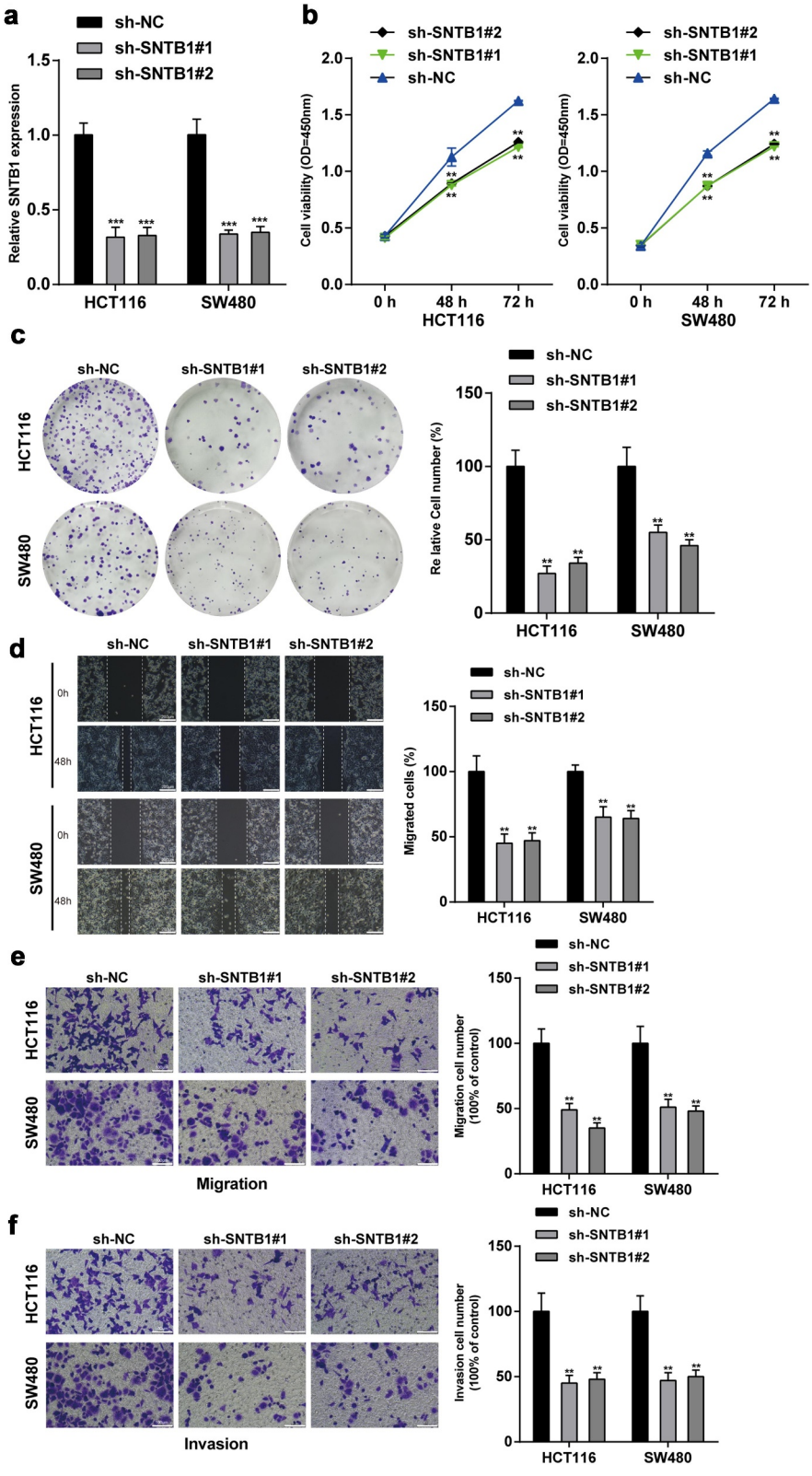

Figure 4. Effects of SNTB1 knockdown on colorectal cancer cell phenotypes (a) SNTB1 knockdown was achieved in target cells by transfecting short hairpin RNA targeting SNTB1 (sh-SNTB1#1/2); SNTB1 expression was determined using Qrt-PCR for confirmation. Subsequently, HCT116 and SW480 cells were transduced with sh-SNTB1#1/2 and examined for cell viability using CCK-8 assay (b); colony formation (c); cell migration using wound healing assay (d); cell migration using Transwell assay (e); cell invasion using Transwell assay (f).

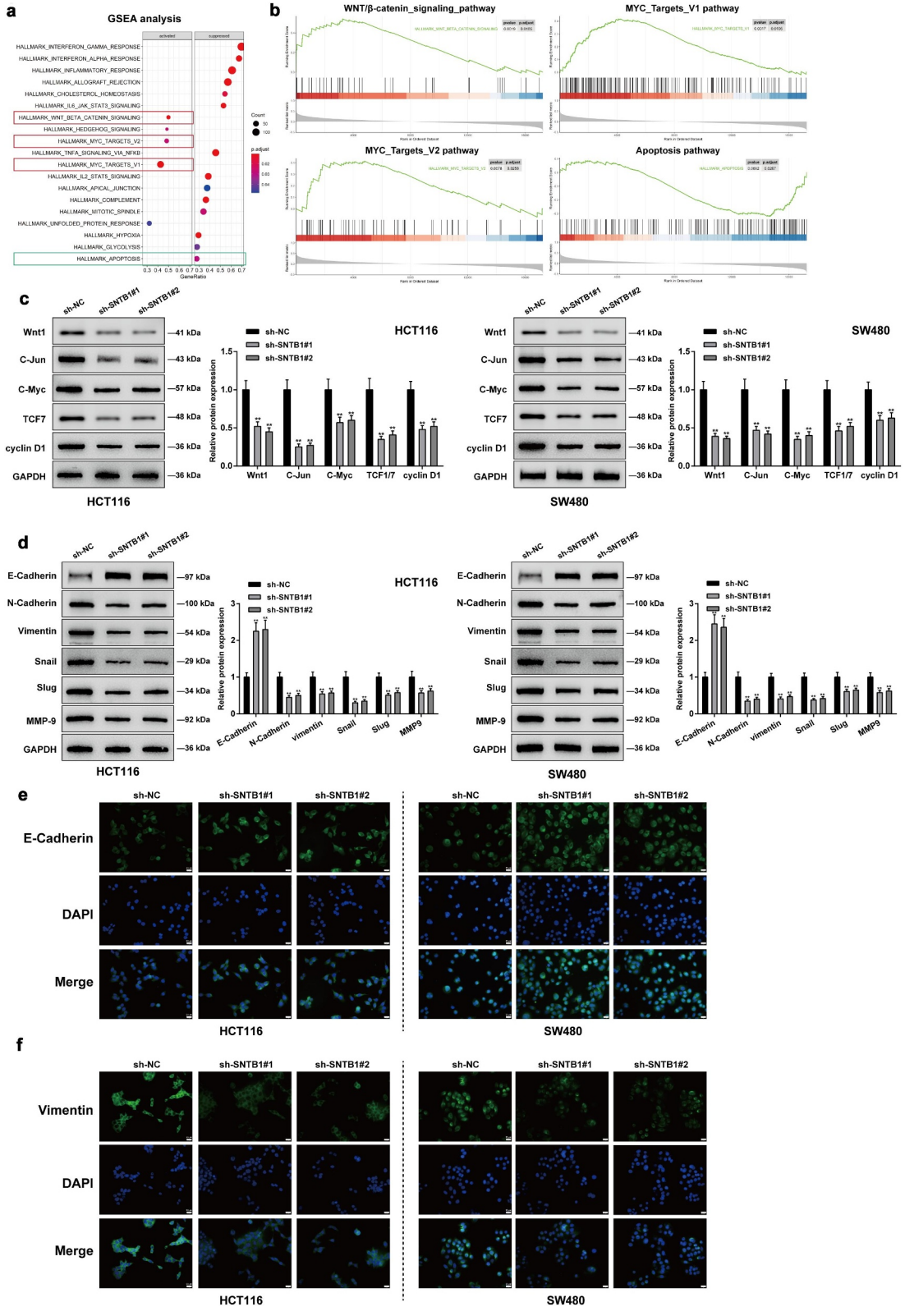

Figure 5. SNTB1 modulates the Wnt/β-catenin/MYC signaling and epithelial–mesenchymal transition (EMT) (a) the correlation between SNTB1 expression and 20,530 genes in the TCGA-COADREAD expression matrix containing 434 samples was analyzed using the R language PSYCH package. The statistical method was Pearson's correlation analysis. (b) Gene set data were downloaded from misgdb (https://www.Gsea-msigdb.Org/gsea/msigdb/index.jsp) and GSEA analysis was performed with the clusterProfiler package using the cancer signature gene set hallmark (h.All.v7.2.entrez.gmt). Subsequently, HCT116 and SW480 cells were transduced with sh-SNTB1#1/2 and examined for the protein levels of the Wnt/β-catenin/MYC signaling factors, Wnt1, C-Jun, C-Myc, TCF7, and cyclin D1 using Immunoblotting (c); the protein levels of EMT markers, E-cadherin, N-cadherin, Vimentin, Snail, Slug, and MMP-9 using Immunoblotting (d); the levels and distribution of E-cadherin and Vimentin using Immunofluorescent staining (IF) (e-f).

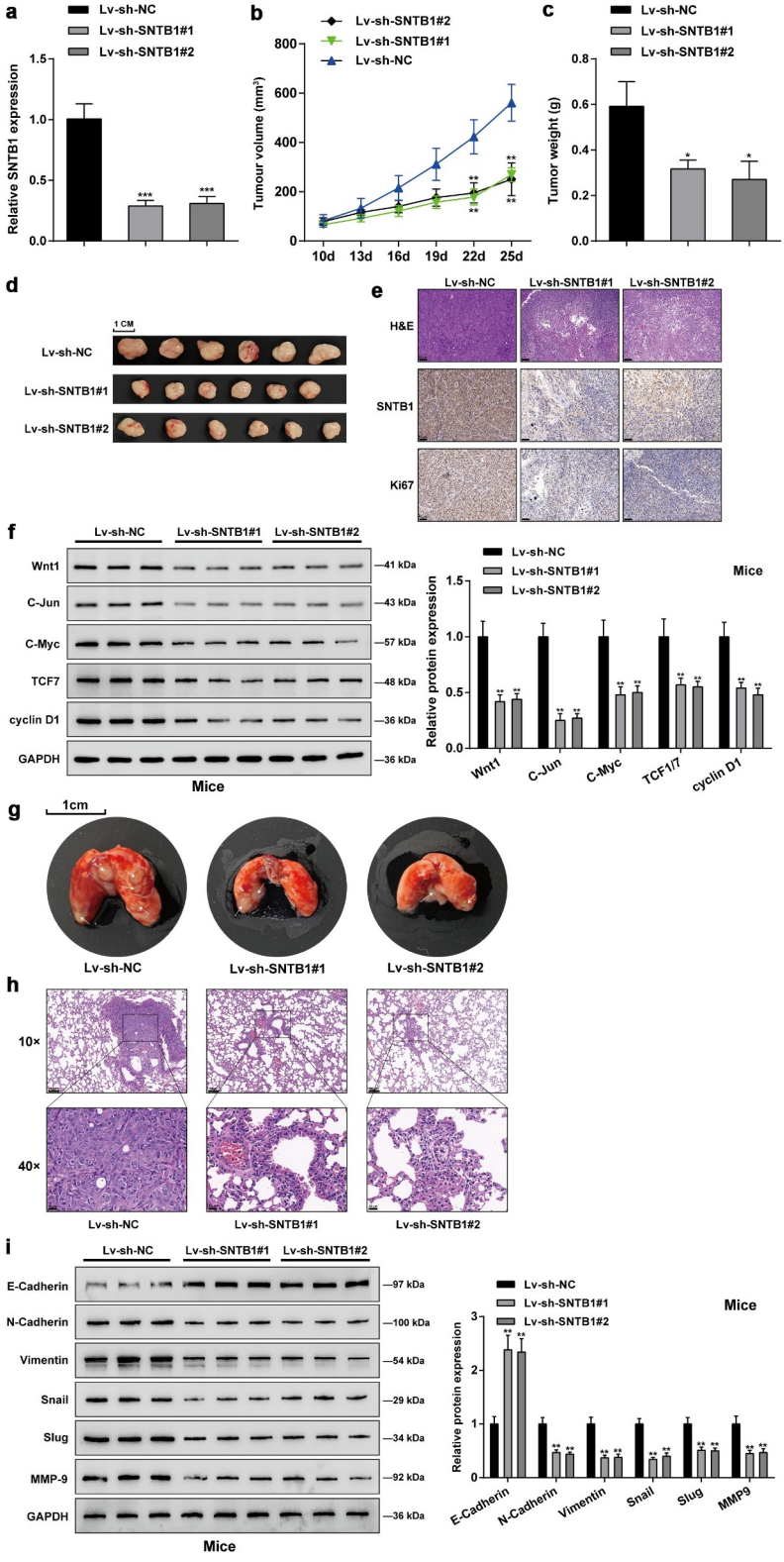

Figure 6. *In vivo* effects of SNTB1 on tumor growth and metastasis in mice models Subcutaneous xenotransplanted tumor model was established in nude mice by injecting HCT116 cells transduced with Lv-sh-NC or Lv-sh-SNTB1#1/2 and examined for SNTB1 knockdown using Qrt-PCR (a); tumor volume and weight (b-c); tumor morphology (d); histopathological characteristics by H&E staining and the levels of SNTB1 and Ki67 in tissue samples by IHC staining (e); the protein levels of Wnt1, C-Jun, C-Myc, TCF7, and cyclin D1 in tissue samples using Immunoblotting (f). Metastatic tumor model was established by tail vein injection of HCT116 cells transduced with Lv-sh-NC or Lv-sh-SNTB1#1/2 and examined for metastatic foci number in lungs (g); histopathological characteristics by H&E staining (h); the protein levels of EMT markers, E-cadherin, N-cadherin, Vimentin, Snail, Slug, and MMP-9 using Immunoblotting (i).

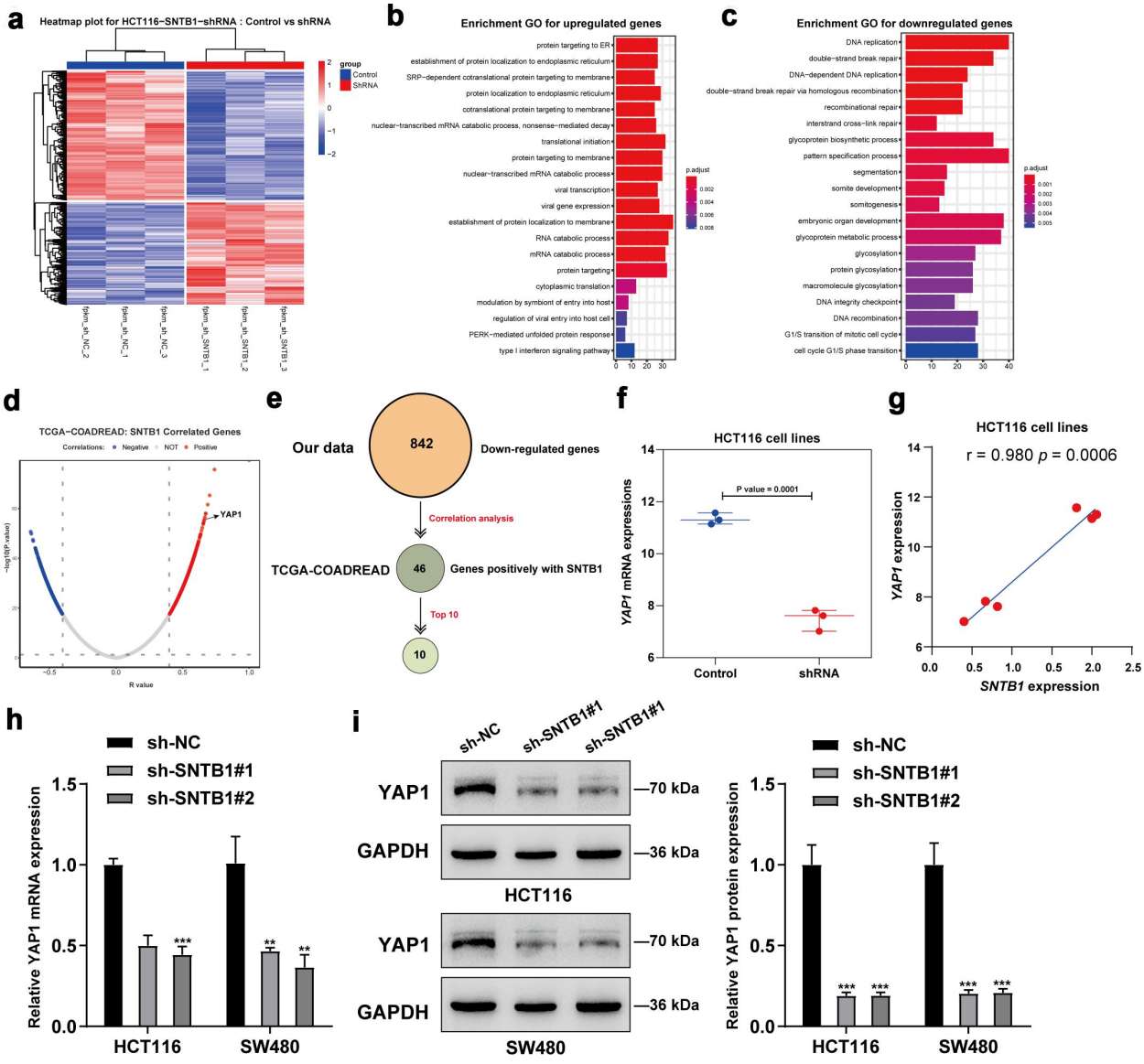

Figure 7. YAP1 mediates SNTB1 functions on colorectal cancer cells HCT116 cells were transduced with sh-SNTB1#1/2 and applied for RNA-sequencing identifying altered protein-coding RNAs. (a) the DEseq2 analysis package of the R language was used to analyze DEGs based on detected protein-coding mRnas, and thresholds were set as log2FC > 0.4 or <-0.4 and $P < 0.05$. (b-c) the Clusterprofiler package of the R language was used for functional enrichment analysis of up-regulated and down-regulated DEGs. (d) Expression profiles from TCGA-COADREAD (Tcga.Coadread.samplemap_hiseqv2.gz) were used to identify SNTB1-associated genes using the psych package of the R language and Pearson's correlation analysis. (e) Diagram of screening process: among 842 down-regulated genes in sh-SNTB1-transduced HCT116 cells, 46 genes exhibited a positive correlation with SNTB1 according to TCGA-COADREAD. The top 10 genes that were significantly positively correlated with SNTB1 were obtained. (f) YAP1 mRNA expression in sh-SNTB1#1- or sh-NC-transduced HCT116 cells. (g) the correlation between YAP1 and SNTB1 expression in sh-SNTB1#1- or sh-NC-transduced HCT116 cells. (H-I) HCT116 and SW480 cells were transduced with sh-SNTB1#1/2 and examined for the mRNA expression and protein levels of YAP1 using Qrt-PCR and Immunoblotting.

with Lv-sh-NC or Lv-sh-SNTB1#1/2. Figure 6g shows that SNTB1 knockdown significantly reduced the number of metastatic foci in lungs, which was further evidenced by the histopathological characteristics revealed by H&E staining (Figure 6h). Regarding EMT, the protein levels of EMT markers were evaluated in metastatic foci; Fig 6l shows that SNTB1 knockdown significantly up-regulated E-cadherin but down-regulated N-cadherin, Vimentin, Snail, Slug,

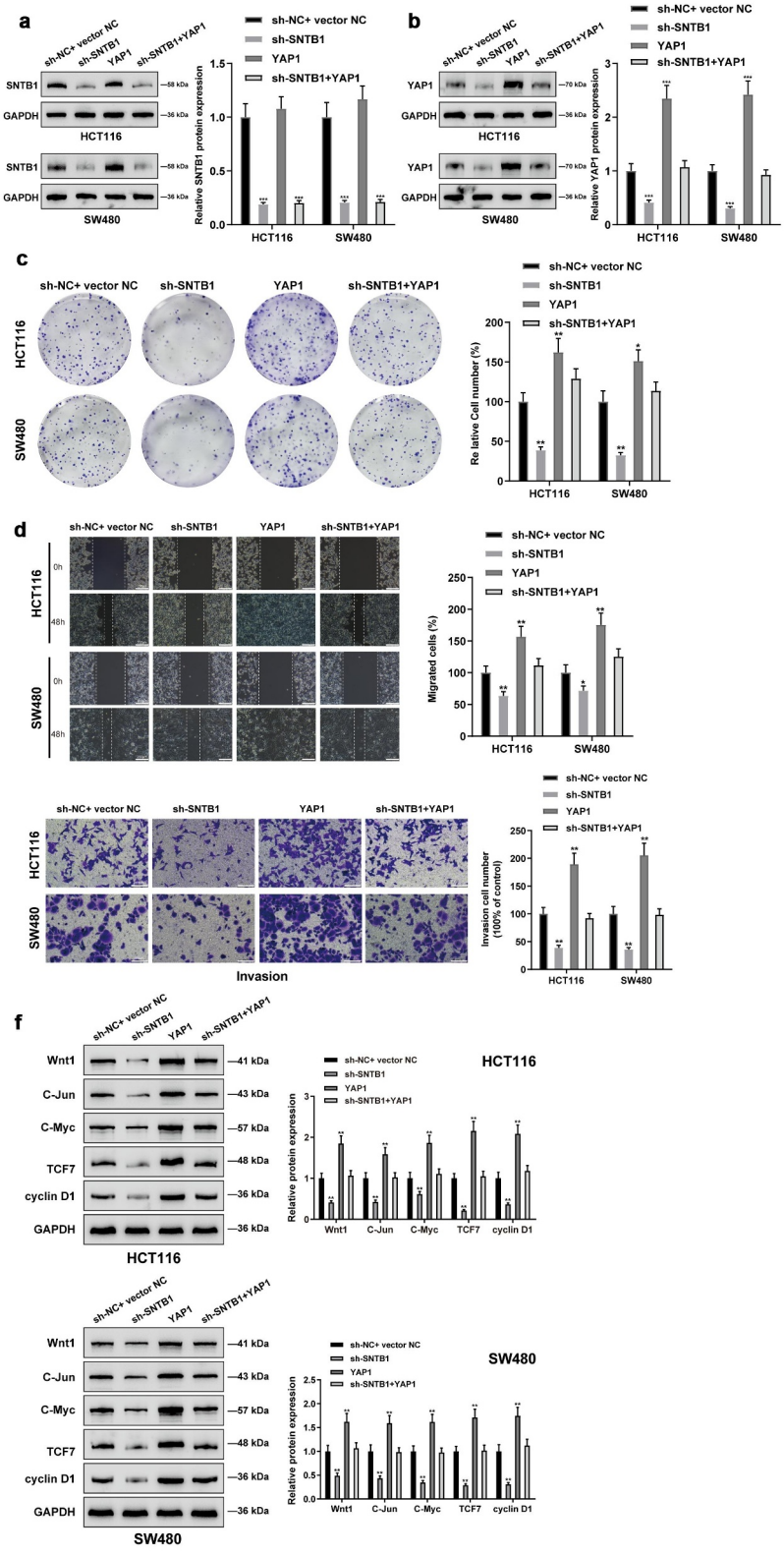

Figure 8. Dynamic effects of SNTB1 and YAP1 on colorectal cancer cell phenotypes HCT116 and SW480 cells were co-transduced with sh-SNTB1 and YAP1-overexpressing plasmid (YAP1) and examined for the protein levels of SNTB1 (a) and YAP1 (b) using Immunoblotting; colony formation (c); cell migration using wound healing assay (d); cell invasion using Transwell assay (e); the protein levels of Wnt1, C-Jun, C-Myc, TCF7, and cyclin D1 using Immunoblotting (f).

and MMP-9 protein contents. These data indicate that SNTB1 knockdown suppresses colorectal cancer lung metastasis in mice models.

YAP1 mediates SNTB1 functions on colorectal cancer cells

For investigating downstream molecular mechanism, HCT116 cells were infected with lentivirus sh-NC or sh-SNTB1 and applied for RNA-sequencing identifying altered protein-coding RNAs. Among 17,061 detected genes, by using thresholds of log2FC > 0.4 or <-0.4 and $P < 0.05$, 665 were markedly increased and 842 were decreased within sh-SNTB1-transduced HCT116 cells (Figure 7a). The functional enrichment analysis of increased and decreased DEGs was conducted using the Clusterprofiler package of the R language. Gene Ontology (biological process, BP) analysis shows that increased genes were enriched in ER stress, protein synthesis, and RNA metabolism (Figure 7b), while decreased related genes were enriched in cell cycle regulation and DNA repair (Figure 7c). In summary, SNTB1 exerts a crucial effect on balancing tumor cell stress and cell cycle.

Furthermore, expression profiles from TCGA-COADREAD (TCGA.COADREAD.sampleMap_HiSeqV2.gz) were used to identify SNTB1-associated genes using the psych package of the R language and Pearson's correlation analysis. Fig 7d shows that 1155 genes exhibited a negative correlation ($r < -0.4$, $P < 0.05$), and 959 genes exhibited a positive correlation ($r > 0.4$, $P < 0.05$) with SNTB1. Among 842 down-regulated genes in sh-SNTB1-transduced HCT116 cells, 46 genes exhibited a positive correlation with SNTB1 and 33 genes exhibited a negative correlation with SNTB1 according to TCGA-COADREAD (Figure 7e). The top10 genes that were significantly positively correlated with SNTB1were listed in Table S2. Among the 10 genes, YAP1 has been reported to play a critical role in colorectal cancer [29–32] therefore, YAP1 was chosen for following investigations.

According to RNA-seq data and qRT-PCR analysis, YAP1 mRNA expression was significantly down-regulated in sh-SNTB1#1/2-transduced HCT116 cells (Figure 8f,h). In sh-SNTB1#1- or sh-NC-transduced HCT116 cells, YAP1 and SNTB1 were positively correlated (Figure 7g). Moreover, according to TCGA-COADREAD, GSE8671, GSE106582, GSE74602, GSE9348, GSE44076, and GSE39582, YAP1 and SNTB1 were positively correlated (**Fig S1**). Consistently, in sh-SNTB1#1/2-transduced HCT116 and SW480 cells, YAP1 protein levels were significantly decreased (Figure 7i). These data indicate that in colorectal cancer cells, SNTB1 positively regulates YAP1 expression.

Dynamic effects of SNTB1 and YAP1 on colorectal cancer cell phenotypes

Considering the positive SNTB1 regulation of YAP1, lastly, the dynamic effects of SNTB1 and YAP1 were investigated on the phenotypes of colorectal cancer cells. HCT116 and SW480 cells were co-transduced with sh-SNTB1 and YAP1-overexpressing plasmid (YAP1) and determined for SNTB1 and YAP1 protein contents. Regarding SNTB1 expression, SNTB1 protein levels were decreased by sh-SNTB1 but not altered by YAP1 overexpression; in the meantime, in co-transduced cells, YAP1 overexpression caused no alterations on sh-SNTB1-caused SNTB1 knockdown (Figure 8a). Regarding YAP1 expression, sh-SNTB1 decreased, whereas YAP1 increased YAP1 protein levels; furthermore, the suppressive effects of sh-SNTB1 on YAP1 protein levels were partially eliminated by YAP1 (Figure 8b).

Regarding cellular functions, SNTB1 knockdown inhibited, whereas YAP1 overexpression promoted colorectal cancer cell colony formation (Fig 9C), cell migration (Figure 8d), and cell invasion (Figure 8e); the inhibitory effects of SNTB1 knockdown upon cancer cell aggressiveness were partially eliminated by YAP1 overexpression (Figure 8c-e). Regarding the Wnt/β-catenin/MYC signaling, SNTB1 knockdown decreased, whereas YAP1 overexpression increased Wnt1, C-Jun, C-Myc, TCF7, and cyclin D1 protein contents; the inhibitory effects of SNTB1 knockdown upon the Wnt/β-catenin/MYC pathway-related factors were partially abolished by YAP1 overexpression (Figure 8f). These data indicate that YAP1 mediates SNTB1 functions on colorectal cancer cells.

Discussion

According to integrative bioinformatics analyses based on four datasets, 293 genes were dramatically increased and 369 genes were decreased within colon cancer samples. Among up-regulated genes, top five genes correlated with colorectal cancer patient's prognosis were verified for expression in clinical samples and SNTB1 was the most up-regulated. *In vitro*, SNTB1 knockdown suppresses the malignant behaviors of colorectal cancer cells, including cell viability, colony formation capacity, as well as the abilities to migrate and invade. Furthermore, SNTB1 knockdown decreased the levels of Wnt1, C-Jun, C-Myc, TCF7, and cyclin D1, and inhibited EMT in both cell lines. *In vivo*, SNTB1 knockdown inhibited tumor growth and metastasis in nude mice models. SNTB1 positively regulated YAP1 expression; YAP1 partially reversed the effects of SNTB1 on colorectal cancer cell phenotypes and the Wnt/β-catenin/MYC signaling.

Integrative bioinformatic analyses have been used to identify promising therapeutic targets for cancer treatment regiments, including colorectal cancer. In this study, by performing DEG analysis based on four online datasets, we demonstrated that 293 genes were remarkably increased and 369 genes were decreased within colon cancer samples. Notably, functional enrichment annotation indicated the enrichment of increased genes in tumor proliferation and apoptosis-related pathways, cell cycle, TP53 signaling pathway, and IL-17 family-mediated signaling pathways, which are correlated with cancer cell apoptosis [33] and immunosurveillance escape [28]. Downregulated genes were enriched in metabolic pathways such as nitrogen metabolism, steroid hormone biosynthesis, retinol metabolism, mineral absorption, bile secretion, and pancreatic secretion, indicating the loss of colon functions during colorectal cancer. Among up-regulated genes, SNTB1 attracted attention because its correlation with poor prognosis in patients and dramatic elevated expression. Reportedly, the level of SNTB1 is elevated in colorectal cancer tissue, according to a gene expression profile microarray including DEGs between matched colorectal cancer and non-cancerous tissues [34]. In the meantime, other studies also reported that SNTB1 levels were increased within colorectal cancer tissue samples and cells. The increase in SNTB1 exhibited a positive correlation with the malignancy degree and worse prognosis in colorectal cancer [35,36]. In this study, consistent expression trend of SNTB1 was observed based on integrative bioinformatics analyses on four datasets that SNTB1 expression was dramatically up-regulated in colorectal cancer samples, higher in samples at advanced T/N/M and clinical stages. Furthermore, experimental investigations also saw up-regulated SNTB1 expression in colorectal cancer samples and cell lines, suggesting its potential role in colorectal cancer tumorigenesis.

SNTB1, which belongs to the syntrophin gene family, is primarily expressed in skeletal and smooth muscle, liver, and kidney, while low expression of SNTB1 is observed in a variety of other tissues, including colon tissue [37]. Recent research has linked SNTB1 functional variations to a variety of illnesses, such as acute pancreatitis, oral cancer, pulmonary cancer, and high myopia [38–40]. Although reduced level of SNTB1 showed to be linked to a poorer survival rate within lung adenocarcinoma patients [40], SNTB1 acts as an oncogene in a variety of tumors, including colorectal cancer. Obinata et al. [41] suggested that knockdown of SNTB1 significantly inhibited migration of androgen and androgen receptor (AR)-negative prostate cancer cells. Ji et al. [42] found 21 fusion genes, including MCM4-SNTB1, as the most frequent and significant in thymomas. Liu et al. [36] demonstrated that SNTB1 enhances CRC tumor progression and development, probably through decreasing PKN2 expression and activating the ERK and AKT pathways. Liang et al. [35] revealed that SNTB1 knockdown inhibited tumor development and cancer cell stemness *in vitro*, as well as carcinogenesis *in vivo* via regulating the β-catenin signaling. Consistently, SNTB1 knockdown inhibited colorectal cancer cell aggressiveness, including proliferation, invasion, and migration. As aforementioned, colorectal cancer mortality is mostly caused by treatment failure and distant metastases [43]. In this study, SNTB1 knockdown suppressed tumor growth and lung metastasis in nude mice models, further indicating the critical role of SNTB1 in colorectal cancer tumorigenesis.

Tumor metastasis, one of the most prominent malignant tumor hallmarks, is a complicated and multistep process driven by genetic and epigenetic alterations [44,45]. EMT begins the first stage of tumor cell metastatic dispersion by enhancing cell motility and invasiveness [7]. Notably, abnormal EMT activation has been identified as the main program of human colon cancer [46]. In this study, SNTB1 knockdown also suppressed EMT through up-regulating the expression of epithelial markers like E-cadherin and down-regulating the expression of mesenchymal markers like N-cadherin, Vimentin, Snail, Slug, and MMP-9. Furthermore, SNTB1 knockdown suppressed Wnt/β-catenin/MYC signaling activation, which has been reported as one of the most prominent molecular therapeutic targets for colon cancer [14] because of its critical role in accelerating EMT and facilitating metastatic features of colon cancer [15]. Regarding the downstream molecular mechanism, YAP1 was identified as one of the positively correlated genes with SNTB1. To govern cell growth and organ size, the Hippo-YAP/TAZ signaling has emerged as a hub integrating multiple inputs such as mechanical and cytoskeletal signals, cellular adhesion, apico-basolateral polarity, and mitogens [47,48]. Furthermore, YAP/TAZ are important mediators of the alternative Wnt pathway [49]. More importantly, a β-catenin-YAP1-TBX5 complex was found to be essential for β-catenin-driven cancer transformation and survival [50]. For example, Deng et al. [51] reported that YAP triggers the Wnt/β-catenin pathway and promotes enterocyte self-renewal, regeneration, and tumorigenesis after DSS-induced injury. Kim et al. [52] found that Wnt/β-catenin signaling activation suppressed hepatocellular carcinoma formation by inhibiting the positive feedback loop between YAP/TAZ and Notch signaling. In this study, SNTB1 positively regulated YAP1 expression but YAP1 overexpression failed to alter SNTB1 expression, suggesting that YAP1 is downstream of SNTB1. Moreover, YAP1 overexpression significantly eliminated the anti-tumor effects of SNTB1 knockdown on colorectal cancer cell aggressiveness and Wnt signaling activation, indicating that YAP1 mediates the functions of SNTB1 on colorectal cancer [53–58].

In conclusion, SNTB1 knockdown inhibits colorectal cancer cell aggressiveness in vitro and tumor growth and metastasis in vivo through the Wnt/β-catenin/MYC signaling; YAP1 might mediate SNTB1 functions on colorectal cancer.

Disclosure statement

No potential conflict of interest was reported by the authors.

Funding

This study was supported by the Foundation of China Hunan Provincial Science & Technology Department (2021SK2001), National Key Research and Development Program of China (2022YFE0134700) and the National Natural Science Foundation of China (51875580).

Ethical approval

All procedures performed in studies involving human participants were in accordance with the ethical standards of Third Xiangya Hospital of Central South University and the 1964 Helsinki declaration. Informed consent to participate in the study has been obtained from participants.

The guidelines for the care and use of animals were carried out according to the Ethics Committee's Guidelines for laboratory animals of Third Xiangya Hospital of Central South University.

Consent for publication

Consent for publication was obtained from the participants.

Data availability statement

The authors confirm that the data supporting the findings of this study are available within the article.

References

[1] Dekker E, Tanis PJ, Vleugels JLA, et al. Colorectal cancer. Lancet. 2019;394(10207):1467–1480. doi: 10.1016/S0140-6736(19)32319-0

[2] Allgayer H, Leupold JH, Patil N. Defining the "Metastasome": Perspectives from the genome and molecular landscape in colorectal cancer for metastasis evolution and clinical consequences. Semin Cancer Biol. 2020;60:1–13. doi: 10.1016/j.semcancer.2019.07.018

[3] Kopetz S, Chang GJ, Overman MJ, et al. Improved survival in metastatic colorectal cancer is associated with adoption of hepatic resection and improved chemotherapy. J Clin Oncol. 2009;27(22):3677–3683. doi: 10.1200/JCO.2008.20.5278

[4] Dongre A, Weinberg RA. New insights into the mechanisms of epithelial–mesenchymal transition and implications for cancer. Nat Rev Mol Cell Biol. 2019;20(2):69–84. doi: 10.1038/s41580-018-0080-4

[5] Aiello NM, Brabletz T, Kang Y, et al. Upholding a role for EMT in pancreatic cancer metastasis. Nature. 2017;547(7661):E7–E8. doi: 10.1038/nature22963

[6] Zavadil J, Bottinger EP. TGF-β and epithelial-to-mesenchymal transitions. Oncogene. 2005;24(37):5764–5774. doi: 10.1038/sj.onc.1208927

[7] Thiery JP, Acloque H, Huang RY, et al. Epithelial-mesenchymal transitions in development and disease. Cell. 2009;139(5):871–890. doi: 10.1016/j.cell.2009.11.007

[8] Bruner HC, Derksen PWB. Loss of E-Cadherin-dependent cell–cell adhesion and the development and progression of cancer. Cold Spring Harb Perspect Biol. 2018;10(3):10. doi: 10.1101/cshperspect.a029330

[9] Lindner P, Paul S, Eckstein M, et al. EMT transcription factor ZEB1 alters the epigenetic landscape of colorectal cancer cells. Cell Death Dis. 2020;11(2):147. doi: 10.1038/s41419-020-2340-4

[10] Hofheinz RD, Stintzing S. Study evidence confirms current clinical practice in refractory metastatic colorectal cancer: the ReDOS trial. Lancet Oncol. 2019;20(8):1036–1037. doi: 10.1016/S1470-2045(19)30390-0

[11] Yuan JH, Yang F, Wang F, et al. A long noncoding RNA activated by TGF-β promotes the invasion-metastasis cascade in hepatocellular carcinoma. Cancer Cell. 2014;25(5):666–681. doi: 10.1016/j.ccr.2014.03.010

[12] Zhang J, Kuang Y, Wang Y, et al. Notch-4 silencing inhibits prostate cancer growth and EMT via the NF-κB pathway. Apoptosis. 2017;22(6):877–884. doi: 10.1007/s10495-017-1368-0

[13] Yang S, Liu Y, Li MY, et al. FOXP3 promotes tumor growth and metastasis by activating Wnt/β-catenin signaling pathway and EMT in non-small cell lung cancer. Mol Cancer. 2017;16(1):124. doi: 10.1186/s12943-017-0700-1

[14] Weng W, Feng J, Qin H, et al. Molecular therapy of colorectal cancer: progress and future directions. Int J Cancer. 2015;136:493–502. doi: 10.1002/ijc.28722

[15] Liu CC, Cai DL, Sun F, et al. FERMT1 mediates epithelial–mesenchymal transition to promote colon cancer metastasis via modulation of β-catenin transcriptional activity. Oncogene. 2017;36(13):1779–1792. doi: 10.1038/onc.2016.339

[16] Polakis P. Casein kinase 1: a Wnt'er of disconnect. Curr Biol. 2002;12(14):R499–R501. doi: 10.1016/S0960-9822(02)00969-7

[17] Grumolato L, Liu G, Haremaki T, et al. β-catenin-independent activation of TCF1/LEF1 in human hematopoietic tumor cells through interaction with ATF2 transcription factors. PLoS Genet. 2013;9(8):e1003603. doi: 10.1371/journal.pgen.1003603

[18] Lu FI, Sun YH, Wei CY, et al. Tissue-specific derepression of TCF/LEF controls the activity of the Wnt/β-catenin pathway. Nat Commun. 2014;5(1):5368. doi: 10.1038/ncomms6368

[19] White BD, Chien AJ, Dawson DW. Dysregulation of Wnt/β-catenin signaling in gastrointestinal cancers. Gastroenterology. 2012;142(2):219–232. doi: 10.1053/j.gastro.2011.12.001

[20] Huang J, Liang X, Xuan Y, et al. A reference human genome dataset of the BGISEQ-500 sequencer. Gigascience. 2017;6(5):1–9. doi: 10.1093/gigascience/gix024

[21] Li R, Li Y, Kristiansen K, et al. SOAP: short oligonucleotide alignment program. Vol. 24. Oxford, England: Bioinformatics; 2008. pp. 713–714.

[22] Kim D, Langmead B, Salzberg SL. HISAT: a fast spliced aligner with low memory requirements. Nat Methods. 2015;12(4):357–360. doi: 10.1038/nmeth.3317

[23] Langmead B, Salzberg SL. Fast gapped-read alignment with Bowtie 2. Nat Methods. 2012;9(4):357–359. doi: 10.1038/nmeth.1923

[24] Li B, Dewey CN. RSEM: accurate transcript quantification from RNA-Seq data with or without a reference genome. BMC Bioinf. 2011;12(1):1–16. doi: 10.1186/1471-2105-12-323

[25] Yu G, Wang L-G, Han Y, et al. clusterProfiler: an R package for comparing biological themes among gene clusters. OMICS. 2012;16(5):284–287. doi: 10.1089/omi.2011.0118

[26] Love MI, Huber W, Anders S. Moderated estimation of fold change and dispersion for RNA-seq data with DESeq2. Genome Bio. 2014;15(12):1–21. doi: 10.1186/s13059-014-0550-8

[27] Abdi H. Bonferroni and Šidák corrections for multiple comparisons. Encycl Meas Stat. 2007;3:103–107.

[28] Wu D, Wu P, Huang Q, et al. Interleukin-17: a promoter in colorectal cancer progression. Clin Dev Immunol. 2013;2013:436307. doi: 10.1155/2013/436307

[29] Ou C, Sun Z, He X, et al. Targeting YAP1/LINC00152/FSCN1 signaling axis prevents the progression of colorectal cancer. Adv Sci. 2020;7(3):1901380. doi: 10.1002/advs.201901380

[30] Ou C, Sun Z, Li X, et al. MiR-590-5p, a density-sensitive microRNA, inhibits tumorigenesis by targeting YAP1 in colorectal cancer. Cancer Lett. 2017;399:53–63. doi: 10.1016/j.canlet.2017.04.011

[31] Chen C, Yuan W, Zhou Q, et al. N6-methyladenosine-induced circ1662 promotes metastasis of colorectal cancer by accelerating YAP1 nuclear localization. Theranostics. 2021;11(9):4298–4315. doi: 10.7150/thno.51342

[32] Sun Z, Zhang Q, Yuan W, et al. MiR-103a-3p promotes tumour glycolysis in colorectal cancer via hippo/YAP1/HIF1A axis. J Exp Clin Cancer Res. 2020;39(1):250. doi: 10.1186/s13046-020-01705-9
[33] Liebl MC, Hofmann TG. The role of p53 signaling in colorectal cancer. Cancers (Basel). 2021;13(9):2125. doi: 10.3390/cancers13092125
[34] Shen A, Chen Y, Liu L, et al. EBF1-mediated upregulation of ribosome assembly factor PNO1 contributes to cancer progression by negatively regulating the p53 signaling pathway. Cancer Res. 2019;79(9):2257–2270. doi: 10.1158/0008-5472.CAN-18-3238
[35] Liang Y, Wang B, Chen S, et al. Beta-1 syntrophin (SNTB1) regulates colorectal cancer progression and stemness via regulation of the Wnt/β-catenin signaling pathway. Ann Transl Med. 2021;9(12):1016. doi: 10.21037/atm-21-2700
[36] Liu L, Chen Y, Lin X, et al. Upregulation of SNTB1 correlates with poor prognosis and promotes cell growth by negative regulating PKN2 in colorectal cancer. Cancer Cell Int. 2021;21:547.
[37] Alessi A, Bragg AD, Percival JM, et al. γ-Syntrophin scaffolding is spatially and functionally distinct from that of the α/β syntrophins. Exp Cell Res. 2006;312(16):3084–3095. doi: 10.1016/j.yexcr.2006.06.019
[38] Ye R, Onodera T, Blanchard PG, et al. β1 syntrophin supports autophagy initiation and protects against cerulein-induced acute pancreatitis. Am J Pathol. 2019;189(4):813–825. doi: 10.1016/j.ajpath.2019.01.002
[39] Khor CC, Miyake M, Chen LJ, et al. Genome-wide association study identifies ZFHX1B as a susceptibility locus for severe myopia. Hum Mol Genet. 2013;22(25):5288–5294. doi: 10.1093/hmg/ddt385
[40] Galvan A, Frullanti E, Anderlini M, et al. Gene expression signature of non-involved lung tissue associated with survival in lung adenocarcinoma patients. Carcinogenesis. 2013;34(12):2767–2773. doi: 10.1093/carcin/bgt294
[41] Obinata D, Funakoshi D, Takayama K, et al. OCT1-target neural gene PFN2 promotes tumor growth in androgen receptor-negative prostate cancer. Sci Rep. 2022;12(1):6094. doi: 10.1038/s41598-022-10099-x
[42] Ji G, Ren R, Fang X. Identification and characterization of non-coding RNAs in thymoma. Med Sci Monit. 2021;27:e929727. doi: 10.12659/MSM.929727
[43] Kassahun WT. Unresolved issues and controversies surrounding the management of colorectal cancer liver metastasis. World J Surg Oncol. 2015;13(1):61. doi: 10.1186/s12957-014-0420-6
[44] Gupta GP, Massague J. Cancer metastasis: building a framework. Cell. 2006;127(4):679–695. doi: 10.1016/j.cell.2006.11.001
[45] Tiwari N, Tiwari VK, Waldmeier L, et al. Sox4 is a master regulator of epithelial-mesenchymal transition by controlling Ezh2 expression and epigenetic reprogramming. Cancer Cell. 2013;23(6):768–783. doi: 10.1016/j.ccr.2013.04.020
[46] Loboda A, Nebozhyn MV, Watters JW, et al. EMT is the dominant program in human colon cancer. BMC Med Genomics. 2011;4(1):9. doi: 10.1186/1755-8794-4-9
[47] Pan D. The hippo signaling pathway in development and cancer. Dev Cell. 2010;19(4):491–505. doi: 10.1016/j.devcel.2010.09.011
[48] Wang M, Dai M, Wang D, et al. The regulatory networks of the Hippo signaling pathway in cancer development. J Cancer. 2021;12(20):6216–6230. doi: 10.7150/jca.62402
[49] Park HW, Kim YC, Yu B, et al. Alternative wnt signaling Activates YAP/TAZ. Cell. 2015;162(4):780–794. doi: 10.1016/j.cell.2015.07.013
[50] Rosenbluh J, Nijhawan D, Cox AG, et al. β-catenin-driven cancers require a YAP1 transcriptional complex for survival and tumorigenesis. Cell. 2012;151(7):1457–1473. doi: 10.1016/j.cell.2012.11.026
[51] Deng F, Peng L, Li Z, et al. YAP triggers the Wnt/β-catenin signalling pathway and promotes enterocyte self-renewal, regeneration and tumorigenesis after DSS-induced injury. Cell Death Dis. 2018;9(2):153. doi: 10.1038/s41419-017-0244-8
[52] Kim W, Khan SK, Gvozdenovic-Jeremic J, et al. Hippo signaling interactions with Wnt/β-catenin and Notch signaling repress liver tumorigenesis. J Clin Invest. 2017;127(1):137–152. doi: 10.1172/JCI88486
[53] Diakos CI, Charles KA, McMillan DC, et al. Cancer-related inflammation and treatment effectiveness. Lancet Oncol. 2014;15(11):e493–503. doi: 10.1016/S1470-2045(14)70263-3
[54] Crusz SM, Balkwill FR. Inflammation and cancer: advances and new agents. Nat Rev Clin Oncol. 2015;12(10):584–596. doi: 10.1038/nrclinonc.2015.105
[55] Abron JD, Singh NP, Murphy AE, et al. Differential role of CXCR3 in inflammation and colorectal cancer. Oncotarget. 2018;9(25):17928–17936. doi: 10.18632/oncotarget.24730
[56] Ishihara H, Hara T, Aramaki Y, et al. Interaction of recombinant human interferon-.GAMMA. With liposomes. Chem Pharm Bull (Tokyo). 1991;39(6):1536–1539. doi: 10.1248/cpb.39.1536
[57] Jain RK, Stylianopoulos T. Delivering nanomedicine to solid tumors. Nat Rev Clin Oncol. 2010;7(11):653–664. doi: 10.1038/nrclinonc.2010.139
[58] Liscovsky MV, Ranocchia RP, Gorlino CV, et al. Interferon-γ priming is involved in the activation of arginase by oligodeoxinucleotides containing CpG motifs in murine macrophages. Immunology. 2009;128(1pt2):e159–69. doi: 10.1111/j.1365-2567.2008.02938.x